Author(s): Koivuniemi, Jaakko & Luusalo, Reeta & Hakonen, Pertti J.

Title: Bipolar programmable current supply for superconducting nuclear magnetic resonance magnets

Year: 1998

Version: Final published version

Please cite the original version:

Koivuniemi, Jaakko & Luusalo, Reeta & Hakonen, Pertti J. 1998. Bipolar programmable current supply for superconducting nuclear magnetic resonance magnets. Review of Scientific Instruments. Volume 69, Issue 9. 3418-3425. ISSN 0034-6748 (printed). DOI: 10.1063/1.1149109

AIP | Review of Scientific Instruments

Bipolar programmable current supply for superconducting nuclear magnetic resonance magnets

Jaakko Koivuniemi, Reeta Luusalo, and Pertti Hakonen

Citation: Review of Scientific Instruments **69**, 3418 (1998); doi: 10.1063/1.1149109
View online: http://dx.doi.org/10.1063/1.1149109
View Table of Contents: http://scitation.aip.org/content/aip/journal/rsi/69/9?ver=pdfcov
Published by the AIP Publishing

Bipolar programmable current supply for superconducting nuclear magnetic resonance magnets

Jaakko Koivuniemi,[a] Reeta Luusalo, and Pertti Hakonen
Low Temperature Laboratory, Helsinki University of Technology, P.O. Box 2200, FIN-02015 HUT, Finland

(Received 27 January 1998; accepted for publication 15 June 1998)

In high resolution continuous-wave nuclear magnetic resonance (NMR) work well-reproducible, linear sweeps of current are needed. We have developed a microcontroller based programmable current supply, tested with superconducting magnets with inductance of 10 mH and 10 H. We achieved a resolution and noise of 4 ppm. The supply has an internal sweep with programmable ramping rate and a possibility for remote operation from a computer with either GPIB or RS232 interface. It is based on an 18-bit D/A converter. The maximum output current is ± 10 A, the sweep rate can be set between 1 μA/s–140 mA/s, and the maximum output voltage is ± 2.5 V. In work at ultralow temperatures, especially in superconducting quantum interference device NMR, all rf interference to the experiment should be avoided. One of the sources of this kind of unwanted input is the digital switching noise of fast logic devices. We discuss this problem in the context of our design. © *1998 American Institute of Physics.* [S0034-6748(98)01509-3]

I. INTRODUCTION

A conducting sample or a metallic part of the cryostat at ultralow temperature will heat up if a rapidly changing magnetic field induces eddy currents in it. To minimize this heat leak, only slow field sweeps are used in ordinary nuclear magnetic resonance (NMR) experiments. Such slowly changing currents can be created either with a digital or analog integrator. The current is never a perfect direct current: it contains noise, ripple from rectifiers, and possibly rf interference. All of these will produce heating and may interfere with the operation of a sensitive low-temperature amplifier such as a dc superconducting quantum interference device.

A linear analog current supply has only small random fluctuations in its output due to operational amplifiers, feedback resistors, and the reference voltage source.[1] The power is usually taken from the ac mains. This will give rise to ripple in the current and the supply cannot be considered to be an independent and isolated device anymore. Hence, the requirement of low rf interference to the surroundings leads to a rather old fashioned, linear design compared with the modern switching power supplies of high efficiency. Moreover, the analog circuits suffer from nonlinearities (e.g., voltage dependent capacitances) and thermal drifts as well as from difficulties in the reproducibility of the output current (i.e., it is problematic to set again exactly the same value of current). With digital design many of the problems of analog devices can be avoided. In a digital integrator the temperature stability depends on a reference voltage, generated with a temperature compensated integrated circuit, and a resistor ladder network in which the temperature coefficients of the resistors track each other. Both of these are stable on ppm level at normal operation conditions. The linearity of the ladder type D/A converter depends essentially on how well the resistors match each other. The parasitic thermal feedback may also degrade its linearity.

The transistor switches in the ladder network of a D/A converter have to be driven individually in such a way that a linear ramp is seen at the output. This is done using a binary counter. By changing the period of the clock signal for this counter it is possible to change the sweep rate. The clock signal is at low frequency, between 10 mHz and 2 kHz. One possibility to generate it would be to use a programmable logic circuit with a low frequency time base.[2] Instead, we decided to use a simple and fairly slow microcontroller unit (MCU) operating at 2 MHz code execution cycle. The main advantage of this choice is that much of the system complexity can be moved from the hardware side to the software. Thus, the number of components is minimized. The basic complementary metal-oxide semiconductor logic gate takes power only when switching from 0 to 1 or vice versa as there is momentarily a path from the supply voltage to the ground. Hence a low operation frequency reduces greatly the electromagnetic interference (EMI) produced by these current spikes. The MCU can also turn off its clock and go to a ''sleep'' mode when the sweep is stopped and the clock signal is not needed for the digital integrator.

The current has to be sensed in some manner to be able to control it. The simplest and most obvious way is to feed the current through a precision resistor and to measure the voltage across the resistor. However, if the current is high, it will heat up the resistor producing uncertainty in the measurement. It is possible to sense the current inductively, like in the Danfysik high precision supplies for 50–10 000 A currents.[3] In their design the magnetic flux inside a core material is kept zero by compensating it with an opposite, but much smaller current. This small compensation current is measured using a precision resistor. At the very weak current end, counting of single electrons can be employed, although a current standard based on single-electron transistors (SETs)

[a]Electronic mail: jaakko@boojum.hut.fi

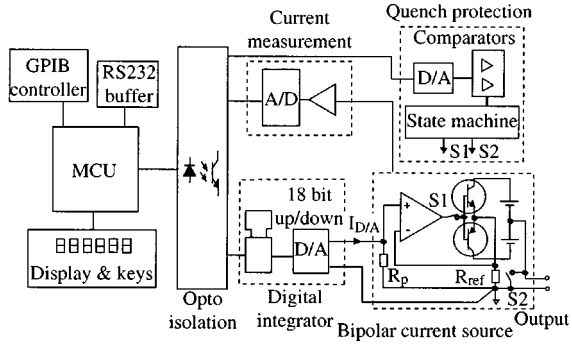

FIG. 1. Block diagram of the current supply. Digital (on the left) and analog parts are separated from each other with optocouplers. The output current is produced by the bipolar current source, which is controlled with the digital integrator. The clock pulses from MCU are used to create linear sweeps of the output current. The comparators and the state machine are used to switch off the output transistors and to shunt the magnet if the output voltage exceeds the value set by the MCU. The output current is monitored by a 20-bit A/D converter.

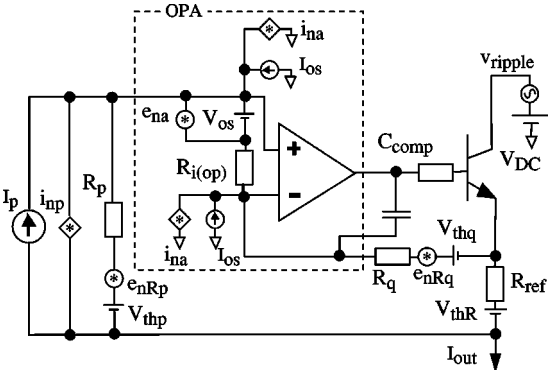

FIG. 2. The constant current source. Only the NPN power transistor (in fact a Darlington pair) is shown for clarity. In the actual bipolar circuit a PNP Darlington is present for negative currents. I_p is the current from the D/A converter. I_{os} and V_{os} are the offset current and voltage of the operational amplifier producing drift to the output current. The input impedance of the operational amplifier is represented with $R_{i(op)}$. Also, thermal voltages V_{thR}, V_{thp}, and V_{thq} due to temperature gradients may become important. The noise seen in the output current comes from the thermal Johnson noises e_{nRq} and e_{nRp} and from the operational amplifier input noise generators e_{na} and i_{na}.

is still under development.[4] The electron pumps based on SETs have already produced a metrological 10^{-8} resolution for currents in the pA range. In the region of our supply $-10-+10$ A, a resistor provides the best solution for reliable operation.

We start by describing the different functional blocks of our design in Sec. II. The nonidealities and expected noise behavior of the current source are evaluated in Sec. III. The digital controller of the supply is described in Sec. IV. A brief description on how to program such a microcontroller is given in Sec. V. The mechanical design of the supply is outlined in Sec. VI. Section VII summarizes the measured noise and stability performance of our supply. The stability was tested with a low temperature NMR experiment. Also an electromagnetic interference measurement is presented in this section.

II. BLOCK DIAGRAM

The current supply can be divided into separate blocks as illustrated in Fig. 1. The digital electronics is isolated from the low noise analog circuitry with seven optocouplers. The MCU does all the ''intellectual'' work needed. Its quartz crystal gives an accurate time base for sweeping the magnetic field. The interrupt handling capability makes it possible to do several things simultaneously. For example the current sweep can operate as a ''background process'' while the user is setting new parameter values from the front panel. Computer interface with RS232 or GPIB is also straightforward to implement.

The analog and mixed (an analog device with digital control of operation) signal functions are (1) digital integrator, (2) bipolar current source, (3) overvoltage (or quench) protection, and (4) current measurement. The digital integrator is made from an 18-bit binary up/down counter and a D/A converter. It has better stability, reproducibility, and linearity than any of the conventional analog integrators made from a capacitor, resistor, and an operational amplifier. Linearity can, however, be deteriorated by thermal feedback effects: A change in the output current gives rise to a change in temperature. The D/A converter DAC729 from Burr–Brown alone would have a linearity better than $\pm 0.0015\%$ of full scale. The bipolar current source is actually a current-in/current-out amplifier. The feedback signal to the operational amplifier comes from the reference resistor R_{ref}. The thermal drift of R_{ref} determines in practice the overall drift of the output current. $S1$ is an optical relay to switch off the output transistors and $S2$ is a power metal-oxide semiconductor field-effect transistor switch to shunt the magnet. These are automatically controlled by a logic circuit forming a simple state machine (see Sec. IV E). The purpose of the state machine is to guarantee a smooth connection of the current supply output to the magnet. The high gain current source might otherwise momentarily try to push current through the magnet and cause a quench when the magnet wires are just being connected. Also, in the case of overvoltage the magnet is shunted immediately with the quickly acting relay $S2$. Subsequently the output transistors are switched off by $S1$. The current measurement is done using the same R_{ref} that is employed to control the current. The A/D converter timing comes from a separate 32.768 kHz clock crystal.

III. CURRENT SOURCE

A. Operation

The operational amplifier (OPA) (see Fig. 2) in the constant current source tries to keep its inputs at the same voltage. It forces a current $I_{\mathrm{out}}=V_{\mathrm{in}}/R_{\mathrm{ref}}$ to flow through the resistor R_{ref} to compensate the voltage created by the D/A converter output on R_p. The output of the D/A converter is taken as a current I_p to make the control more immune to thermal or induced voltages. Since the full scale output is only ± 1 mA, the step size is very small: $2\ \mathrm{mA}/2^{18}=7.6$ nA. Thus, well-planned layout is crucial and leakage currents should be kept well below this value. The current source,

viewed as a current amplifier, has then a gain $A=R_p/R_{\mathrm{ref}}=10^4$ using $R_p=100\ \Omega$ and $R_{\mathrm{ref}}=0.01\ \Omega$.

The real physical OPA can be modeled with an ideal one with external voltage and current sources to account for its drift and noise. These are marked by e_{na}, i_{na}, V_{os}, and I_{os} in Fig. 2. The offset voltage and current are mainly deteriorating the stability, otherwise they could be neglected. We are not concerned on the absolute accuracy. The lowest noise can be obtained with an operational amplifier optimized for low input impedances. We selected Linear Technology LT1028, which has $e_{\mathrm{na}}=1.0\ \mathrm{nV}/\sqrt{\mathrm{Hz}}$ at 10 Hz, $i_{\mathrm{na}}=5\ \mathrm{pA}/\sqrt{\mathrm{Hz}}$ at 10 Hz, $\Delta V_{\mathrm{os}}/\Delta T=0.2\ \mu\mathrm{V}/^{\circ}\mathrm{C}$, and $\Delta I_{\mathrm{os}}/\Delta T=0.1\ \mathrm{nA}/^{\circ}\mathrm{C}$. The resistors cause also noise and may produce thermal voltages due to a temperature difference between two dissimilar metal joints. A dominant pole compensation ($R_q=100\ \Omega$ and $C_{\mathrm{comp}}=22\ \mathrm{nF}$) was used to guarantee the stability of the circuit. This limits the operation bandwidth of the current source to 70 kHz. Susceptibility to oscillations in the frequency range of 100–300 kHz was observed even with the compensation described.

The rejection of ripple or noise voltage v_{ripple} from the voltage source V_{DC} of the current regulator is governed by the common mode rejection ratio of the operational amplifier. At low frequencies up to 200 Hz this is typically 126 dB for LT1028. Thus, the output current ripple is $i_{\mathrm{ripple}}=v_{\mathrm{ripple}}/(R_{\mathrm{ref}}\times CMRR)$. The voltage V_{DC} could be taken from a battery to eliminate any ripple and noise in the raw supply. In practice it was made using a voltage regulator and rectified, filtered ac voltage. For a filter capacitor C the ripple voltage can be estimated to be $v_{\mathrm{ripple}}=I/f\times C$. Here I is the loading current and f the ripple frequency (100 Hz for full wave rectifier). In our case we used a large capacitor $C=0.1$ F giving $v_{\mathrm{ripple}}=1\ V_{\mathrm{pp}}$ at 10 A current. From this we can estimate fluctuations in output current $i_{\mathrm{ripple}}=50\ \mu\mathrm{A_{pp}}$ without any voltage preregulation. In practice the operational amplifier does not see the same common-mode voltages at both of its inputs and the ripple is larger. Thus, a voltage regulator was used in front of the current source.

B. Output noise and drift

Calculation of the output noise is straightforward on the basis of the model in Fig. 2. The most essential noise sources are at the input of the high gain operational amplifier. We get for the output noise

$$i_{\mathrm{nout}}^2=\frac{e_{\mathrm{na}}^2+i_{\mathrm{na}}^2R_p^2+i_{\mathrm{na}}^2R_q^2+i_{\mathrm{np}}^2R_p^2+e_{\mathrm{nRp}}^2+e_{\mathrm{nRq}}^2}{R_{\mathrm{ref}}^2}.$$

The noise in 0.1–10 Hz band is the most important for a dc magnetic field. Higher frequencies are usually rejected by the inductance of the magnet or are not sensed by the averaging lock-in amplifier used for cw NMR detection. At $f<0.1$ Hz the overall system stability and $1/f$ noise determine the fluctuations. These questions are addressed in the context of stability (see Sec. VII). Typical equivalent input noise voltage e_{na} and current i_{na} sources for LT1028 are $6\ \mathrm{nV_{rms}}$ and $100\ \mathrm{pA_{rms}}$ in this frequency range. The latter produces a voltage of $10\ nV_{\mathrm{rms}}$ over R_p. The thermal noise from R_q and R_p is small compared to their excess noise at low frequency.[5] A typical noise index of -20 dB gives 0.1 μV noise (per one volt drop) over one decade of frequency. Since the voltage over R_p and R_q is at most 0.1 V we get for the bandwidth 0.1–10 Hz a value of $15\ \mathrm{nV_{rms}}$. The current noise from DAC729 is probably dominated by $1/f$ noise from its internal voltage reference. The $i_{\mathrm{np}}=0.6\ \mathrm{nA_{pp}}$ transforms into $60\ \mathrm{nV_{pp}}$ at the operational amplifier input. Thus we get an estimate for the output noise current $i_{\mathrm{nout}}=6\ \mu\mathrm{A_{pp}}$. The noise from the other sources (e_{na}, i_{na}, e_{nRp}, and e_{nRq} in Fig. 2) gives $2.7\ \mu\mathrm{A_{rms}}$ or $16\ \mu\mathrm{A_{pp}}$. The total noise current is then $17\ \mu\mathrm{A_{pp}}$. Since the absolute value of the noise and the maximum output current depend on the selection of R_{ref}, it is better to express these noises as ppm of the full scale output. We get a peak-to-peak value of less than 1 ppm.

The thermal drift of the current is due to a change in offset voltage V_{os}, in D/A converter output I_p, in the resistance of R_p, R_q, and R_{ref}, and in thermal EMFs V_{thR}, V_{thp}, and V_{thq}. A small change in input offset current I_{os} is not crucial if both of the operational amplifier inputs see the same impedance. The D/A converter contributes 2 ppm/°C to the drift. The drift due to ΔV_{os} is 1 ppm/°C. The R_p and R_q are Welwyn precision wire wound resistors and have a temperature coefficient of 15 ppm/°C. The R_{ref} is made from a thin Constantan plate (see Sec. VI) and has a typical temperature coefficient of 50 ppm/°C. The thermal voltages can be of order of 1 μV/°C giving rise to 5 ppm/°C drift. Thus the total thermal stability of the output current is in the worst case 100 ppm/°C, mainly determined by the R_{ref}. The temperature of the critical components should be kept constant within 1 °C. Temperature gradients giving rise to differences in thermal voltages should be eliminated as well.

IV. DIGITAL DESIGN

A. Microcontroller and its parallel ports

The heart of the digital electronics is a microcontroller MC68HC711KA4.[6] The internal 24 kbytes of erasable programmable read-only memory (EPROM) for program and 768 bytes of RAM for variables are quite sufficient for our small controller application. The microcontroller has several ways to control the operation of external devices and to read data from them. These devices can be mapped to the MCUs memory, so that the CPU can communicate with them using simple read and write operations. In our case, however, we wanted to avoid this in order to keep all fast signals inside the microcontroller chip to reduce switching noise. There are eight built-in parallel ports (PA–PH),[6] which can be used to pass data. Some of their pins can alternatively be used for other, more sophisticated control or communication operations. The serial peripheral interface moves data between the MCU and an external device as a stream of clocked bits. The timing functions of the microcontroller can be configured to have an external input or output.

Most of the needed digital functions are already implemented in MCUs architecture. The user just has to take care of a few registers in short, interrupt-driven code segments to master the different control operations for external devices. For example, the MCU has a complete interrupt-driven asynchronous serial interface built in. Only one external inte-

grated circuit LT1180 from Linear Technology is necessary to translate the TTL-logic levels to the RS232 standard. The external IEEE488-bus controller chip NAT9914[7] is controlled via two of the MCUs 8-bit parallel ports: PC0–PC7 for data and PF0–PF5 for address and read/write signals. This is acceptable since there is no need for fast transfer of data over the GPIB bus. It also eliminates any external chips that would otherwise be needed, e.g., for address decoding. If the controller chip has received a byte or needs service, it generates an IRQ interrupt to MCU. There are also other interrupts from external sources. The nonmaskable interrupt (XIRQ) is used in the case of an overvoltage across the magnet, which is detected by the voltage comparators. An integrated circuit Maxim MAX690 keeps the RESET signal of the MCU low until the 5 V power supply is stable. The same circuit feeds also current to MCUs internal RAM from a lithium battery when power is lost. Thus, the set values of current and sweep rate are kept in the memory even after the device has been switched off.

There are several parameters (e.g., the sweep rate) that have to be set from the front panel. An optical encoder is used for such a numerical input. Upon rotation it produces two $\pm 90°$ phase shifted square wave signals. The sign of the phase shift depends on the sense of rotation. One of the two signals is used to generate an interrupt pulse accumulator input edge (PAI). The program increases or decreases the value of a variable in the memory depending whether the other input was 0 or 1.

The output current is always displayed in the seven segment numeric displays. They are individually controlled by an 8-bit serial-in-parallel-out register hc595 instead of being driven in sequence (multiplexed) by the MCU. The switching noise is small, since the display is updated only twice a second. The internal control registers of HDSP2503 alphanumeric display from Hewlett-Packard are accessed with two hc595 registers. It has a typical display refresh rate of 256 Hz and takes 0.2–0.4 A of current. To reduce digital noise the alphanumeric display can be kept blank when the parameters are not set.

B. Use of the serial peripheral interface

Many of the new A/D and D/A converters can be operated with synchronous serial interface. Only three lines (clock, data in, and data out) are needed to move arbitrarily many bits of data. Thus the printed circuit board (PCB) can be made smaller and it is easier to design. For isolation between the digital and analog subsystems only four optoisolators are necessary. Although the serial interface is used at a relatively high speed (500 kbits/s) the data transfer happens only at intervals of 64 ms when the A/D converter is read. Thus the switching noise power is reduced to these 30 μs long bursts.

The MCU controls both the display and the current control circuit via the same serial peripheral interface lines (Fig. 3). The distinction between these two is made with a separate latch signal, which loads the sent data either to the display or to the current control board. Reading is done only from the A/D converter (Crystal CS5506 20-bit $\Sigma\Delta$ converter) in the current control board to measure output current or voltage. The 12-bit D/A converter (Maxim MAX538) and a hc595 8-bit serial-in-parallel-out register are connected in series on the current control board. The first sets the maximum output voltage sensed by the comparators. The hc595 is used to select the direction of counting in the digital integrator, for controlling the operation of the A/D converter and to reset the state machine (see Fig. 4) on power-up or after overvoltage.

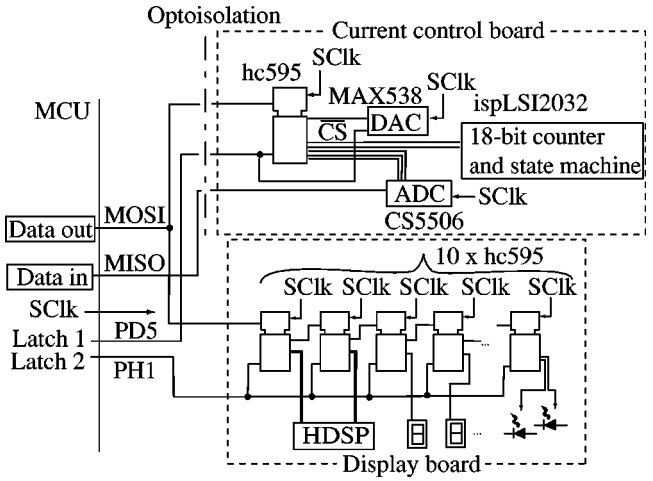

FIG. 3. The serial peripheral interface. The microcontroller ''sees'' peripheral devices through the ''Data out'' and ''Data in'' registers in its address space. The two latch signals are connected to parallel port outputs PD5 and PH1. In the upper part of the figure there are the devices connected to SPI on an optically isolated current control board. The lower part describes the display board.

C. Time based interrupts

All the timing activities are done with the internal counters of the MCU. The heart of these functions is a free running 16-bit counter (TCNT).[6] It was set to the slowest

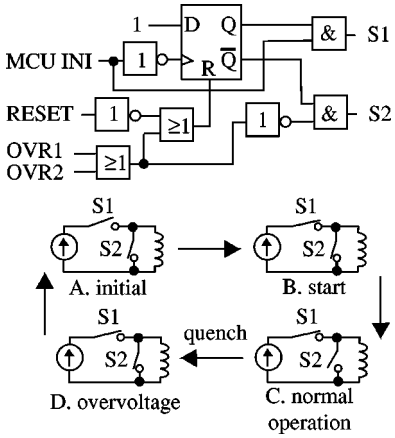

FIG. 4. The state machine drives the switches $S1$ and $S2$ in order to turn on a current to a magnet smoothly or to disconnect the supply when a high voltage is detected. After a system RESET, the state machine is in its initial state *A*. The supply is disconnected and there is a shunt across the magnet. The MCU INI signal is driven low and the machine goes to the state *B*. After MCU INI goes high again, the normal operation *(C)* is reached. Now the shunt is disconnected and the output transistors drive current to the magnet. An overvoltage drives one of the OVRs to 1 and the shunt is closed. Then the comparator does not see the high voltage anymore and OVR goes to 0. The initial state *A* is reached.

TABLE I. List of the interrupts.

Interrupt	Function
Timer output compare 2 (TOC2)	Clock signal for Integrator
Interrupt request (IRQ)	GPIB controller service
Non-maskable interrupt (XIRQ)	Overvoltage
Real time interrupt (RTI)	Read A/D converter and update display
Serial communication interface (SCI)	RS232 communication
Pulse accumulator (PAI)	Edge detected on optical encoder
Clock monitor fail	CPU clock loosing cycles
Computer operating properly failure	Program jammed
Illegal operation code trap	Program mixed up

operation of 8 μs/count. A variable time delay interrupt can be achieved by comparing the TCNT to one of the five comparator registers TOC1–TOC5. If these two match, an interrupt is generated and the corresponding digital output OC1–OC5 changes its state if programmed to do so. The most important use of this mechanism is to generate a variable period clock signal for the digital integrator. The up/down counter of the integrator is increased or decreased with the rising edge of OC2. If the OC2 output is about to make a count in the digital integrator, the upper and lower limits of the current have to be checked. Depending on the function (''Move'' or ''Sweep'') the integrator may have to be stopped or its motion reversed.

A real time interrupt is used to read the A/D converter output at 64 ms intervals. Eight readings are averaged and manipulated before the measured current is displayed. The MCU has an internal RC timer to check that its clock is operating without lost cycles and a software watch dog to make sure that the program has not been jammed to an infinite loop. These are the last three interrupts in Table I.

D. Up/down counter with programmable logic

The synchronous 18-bit up/down counter was implemented with a programmable logic circuit ispLSI2032 from Lattice Semiconductors. It has eight generic logic blocks (GLB). Each of them has four macrocells producing one output. The 18 input signals of the GLB and the outputs of the macrocells can be interconnected in a global routing pool. The GLB has the usual sum-of-products structure with *D*, *T*, or *J-K* type output registers. The circuit can be easily programmed with logic equations. A slow output slew rate can be programmed into the logic circuit. This helps in minimizing the switching noise although it is not very serious problem due to the low clocking frequency.

E. State machine for magnet protection

A simple digital state machine was designed to switch on the output transistors and to close the shunt switch across the magnet. Since this is an essential safety feature it is not wise to rely too much on the proper operation of the complex MCU. An independent logic circuit is used instead. The operating principle of the state machine can be seen in Fig. 4. It was implemented in one of the GLBs of ispLSI2032. It has four inputs: MCU INI, RESET, OVR1, and OVR2. The reset is the global system RESET, which also drives the MCU. MCU INI is generated by the microcontroller to allow for the connection of the supply to the magnet. OVR1 and OVR2 come from two voltage comparators which test the negative and positive limits of the output voltage. The MCU can also disconnect the supply from the magnet by setting the maximum output voltage seen by these comparators to zero. This will produce an overvoltage and the state machine will go to its initial state.

V. PROGRAMMING THE MICROCONTROLLER

The microcontroller can be started in a special bootstrap mode.[6] In this mode a short 256 byte long program is loaded to its memory from an external computer using the RS232 connection. The PCBug11[8] running on a PC can check the operation of the MCU using this program as well as load small test programs to the memory. Programming of the EPROM is possible with the PCBug11. The program for the MCU was written both in C and assembler in a Linux environment. The C compiler was Imagecraft icc11 v. 2.0. The code debugging was done with PcBug11.

The MCU program starts with the initialization of variables together with setting all the I/O pins to a well defined state. The digital integrator is set to zero current. The alphanumeric display, the A/D converter, the D/A converter, and the byte on the current control board are all initialized. The XIRQ interrupt is originally masked after RESET by X-bit in the CPU status register. This mask is cleared with assembly command ''tap'' in microcontroller. After this the mask cannot be set again. The state machine output *S*2 is connected to XIRQ input. Thus the XIRQ interrupt will be generated immediately. The program has a flag to distinguish the initial XIRQ from the overvoltage condition. Now the program moves to the ''con magn'' state. The magnet can be connected to the output terminals safely in this state. The user can run a test, which drives a small slowly increasing <10 mA current through the magnet. If the output voltage stays low enough the test is passed. This is useful in checking the wiring to the magnet and that the superconducting parts are at a low enough temperature for stable operation.

After the output has been connected to the magnet, the program enters the main loop. It will stay forever in this loop checking for different flags. If one of them is set, it will execute the corresponding service routine. Also the parallel port *E* inputs are checked to see if any of the keys has been pressed. The most important interrupt is the time comparator TOC2, which creates the field sweep. The ''Stop/Restart''

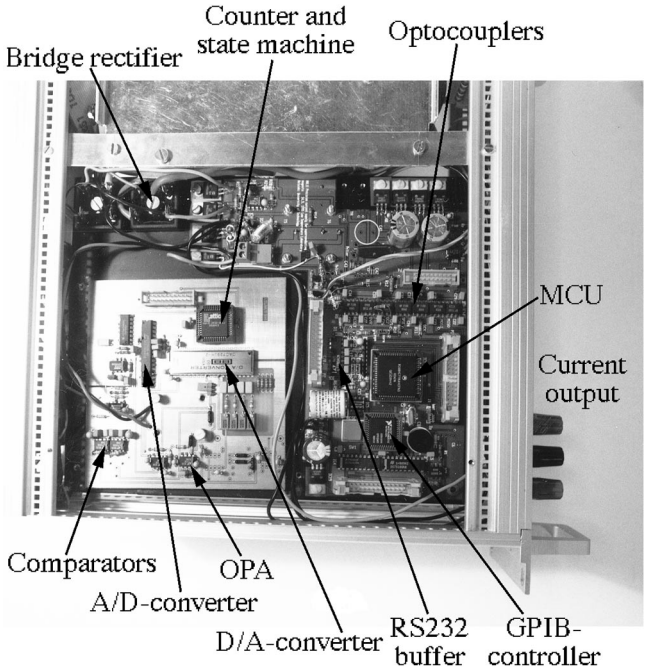

FIG. 5. Current control (lower left corner) and microcontroller boards are shown. The boards are connected together with a ribbon cable, which has been removed for clarity. Also the current control board is shielded with a separate aluminum box in normal operation. The display board is hidden behind the front panel on the right (it is below the aluminum frame).

button or command from GPIB or RS232 sets or clears the mask bit of this interrupt. The real time interrupt serving the A/D converter sets a flag telling the main program to update the display. The GPIB or RS232 computer interface is taken care of if an IRQ or SCI interrupt has occurred. This subroutine reads characters into the input buffer or sends the next character to the external computer. After the routine finds an end-of-command character (carriage return 0x0D or new line 0x0A) the command is interpreted and the corresponding code is executed in the main program.

VI. MECHANICAL DESIGN

Several things have to be kept in mind in the design of an overall layout of the actual current supply. First, the two regulator transistors in series (one for voltage and one for current regulation) are operated in full linear mode, and these dissipate $6\ \mathrm{V}\times 10\ \mathrm{A}=60\ \mathrm{W}$ of power at maximum. This amount of heat has to be carried away by a relatively large heat sink with a thermal resistance of $0.33\ ^\circ\mathrm{C/W}$ to ambient air. Three PCBs were used as seen in Fig. 5. The first one contains all the front panel circuits: the alphanumeric display, the seven segment displays, light-emitting diodes (LEDs), and the keys. The display board was mounted behind the aluminum plate of the front panel.

The most sensitive part of the supply is the current controlling network. It is placed on a separate PCB, which is closed inside a metallic enclosure. This decouples the board from electric interferences and also makes it possible to control the temperature of the circuits. Thus, thermal drifts generated in the D/A converter, the operational amplifier, and the reference resistor can be minimized with respect to the varying dissipation in the power transistors. The reference

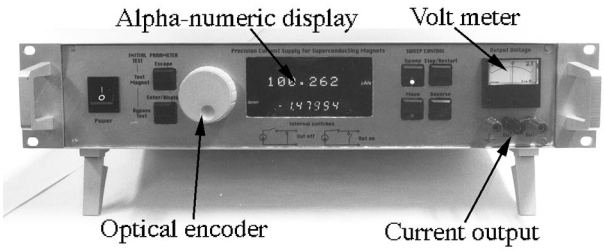

FIG. 6. The front panel of the current supply. The small seven segment display shows always the measured current. The upper alphanumeric display is used to check and change parameters. The optical encoder is used to give numerical input for destination current, lower and upper bounds of the sweep, sweep rate, maximum output voltage, and GPIB address of the unit. It is also employed to select the desired parameter from a menu. The panel meter measures the voltage at the output.

resistor R_{ref} of the current source was made of Constantan resistance alloy (Cu55/Ni45) from Goodfellows Ltd. The 0.1 mm thick plate ($14\ \mathrm{mm}\times 30\ \mathrm{mm}$) was soldered directly on the bottom side of the PCB. The resistivity of the alloy has a small temperature coefficient, typically less than 50 ppm/°C. A Peltier heat pump (Melcor CP1.4-35-06L) is fixed in direct contact with R_{ref}. It is used to regulate the temperature of this resistor and the rest of the current control board.

The third board accommodates the microcontroller, the optoisolators, and all the voltage or current regulators, and transistors. The last ones have to be kept separate from the current controlling board since their heating would result in a large drift of the set current. A ground plane is used systematically everywhere to reduce the impedance seen by the ground return currents. To guarantee error-free operation of the controller a high quality board with solder masks was found to be necessary.

The standard voltage regulators Motorola 7805, 7905, 7815, and 7915 were laid horizontally. They were fixed with nylon screws and silicone insulating washers to the heat sink after soldering their pins to the PCB. The two power Darlington transistors BDX67 and BDX66 in TO3 case for controlling the current were fixed on a niche milled on the other side of the heat sink. The screws were fitted to holes in the printed circuit board. One of the screws couples the transistor collector to the board. Their emitter and base could be soldered directly to the PCB via the holes on it.

The current supply was assembled into Elma 19 in. aluminum rack, Fig. 6. Two cooling fans guarantee a proper airflow inside the closed case.

VII. CURRENT SUPPLY PERFORMANCE

A. Noise measurements

The noise of the current supply was measured by connecting a $0.1\ \Omega$ resistor to the output terminals and amplifying the ac-coupled voltage using a Stanford Research SR560 preamplifier. The measurement was made differentially with the guard shield connected to the ground of SR560. The bandwidth was set to 0.1–10 Hz. A chart recorder Goerz SE120 was used to measure the peak-to-peak noise as illustrated in Fig. 7. When the supply was off, a noise of $9\ \mu\mathrm{A_{pp}}$ was measured in the 0.1–10 Hz band; this is

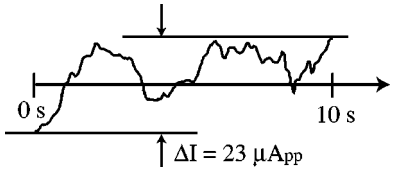

FIG. 7. Noise measurement of the current supply. The output current was 3 A. The peak-to-peak value is roughly six times the root mean square of a Gaussian distributed noise.

the background noise of SR560. The measurement time was limited to 10 s to cut off frequencies lower than 0.1 Hz. The peak-to-peak value of the noise was measured at output currents 0, 1, 2, and 3 A. The corresponding noises were 32, 23, 27, and 23 μA_{pp}. These numbers include also the noise of SR560. They agree quite well with the calculated values and show that the noise is determined by the input equivalent noise of the operational amplifier.

B. Stability

The stability was tested with a cw NMR signal from liquid ^{3}He. The current was kept essentially constant and only a small ramp was produced to measure the sharp NMR line. Thus, the temperature of R_{ref} was almost constant even without a separate temperature control loop. Each field sweep took 5 min. The signal magnitude across a tank circuit was read using a cold preamplifier[9] and a lock-in amplifier PARC 5302. After each NMR reading also the programmed current was read from the supply. The resulting NMR lines are shown in Fig. 8. The minimum in the lock-in amplifier output corresponds to the maximum NMR absorption. The value of the current at the maximum absorption is tabulated in the figure for five sweeps. The fluctuation in the current is ± 70 μA which corresponds to the resolution of the current supply (i.e., 20 A/2^{18}=76 μA).

The frequency stability of the oscillator used for the excitation can be assumed to be much better than the stability of the current supply. Also the resonance frequency of the tank circuit stays constant since the components determining the frequency are inside the cryostat in front of the cryogenic GaAs metal-semiconductor field-effect transistor amplifier.

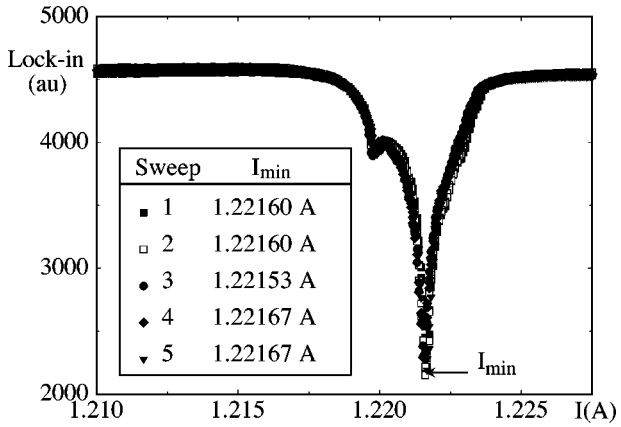

FIG. 8. Five cw NMR signals measured on 0.4 bar liquid ^{3}He at 90 mK. The traces are plotted on top of each other. The insert gives the location of the peak minimum for each sweep. The deviation corresponds to the least significant bit of the D/A converter.

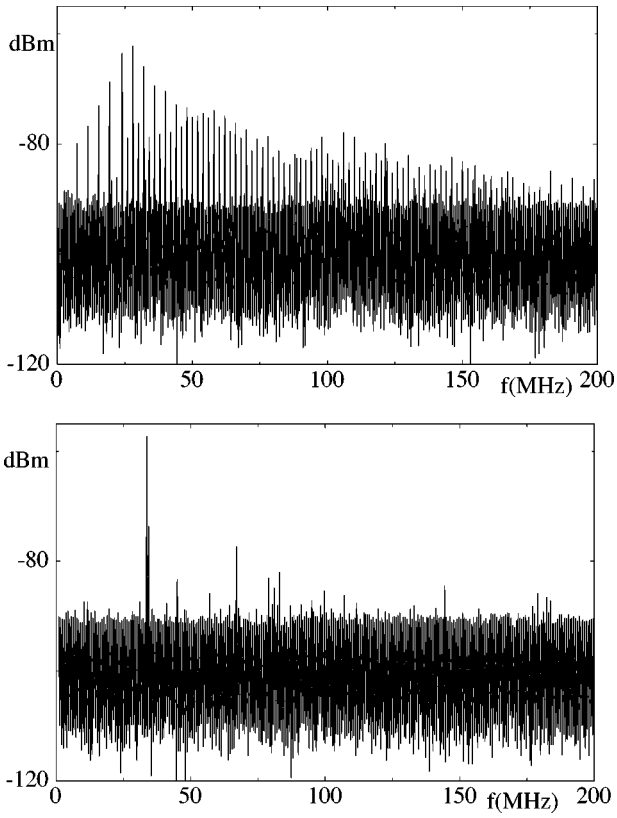

FIG. 9. *Top:* The spectrum of electromagnetic interference produced by the MCU. The trace was measured with a 3 cm diameter loop probe for *H* field (Model 902 from EMCO 7405 near-field probe set). It was 3 cm above the 68 pin PLCC package of the microcontroller. The spectrum analyzer was Hewlett-Packard HP 8562E. Wideband switching noise is visible. The peaks decay quite fast when the probe is moved away from the MCU. They are due to a nonpropagating reactive near field. The highest peak at 30 MHz corresponds to 20 $\mu V/\sqrt{Hz}$ induced to the loop taking into account the 18 dB gain of the probe amplifier. *Bottom:* The interference spectrum when a current of 5 A is driven to a 10 mH superconducting magnet inside a liquid ^{4}He storage dewar. A 4 cm coax loop was placed 8 cm from the magnet. As can be seen, the interference inside the cryostat is small. In fact, the peaks above the noise level remained even when the current supply was switched off.

C. Electromagnetic interference

The heat produced by electromagnetic interference (EMI) is usually due to resistive losses. These can arise from direct conduction of current in a resistive medium (e.g., carbon resistor for temperature measurement) or from induced eddy currents. The heat leak due to eddy currents is proportional to the frequency squared. An alternating magnetic field of 7 pT at 1 MHz gives rise to a 1 μW heat leak to a typical copper nuclear stage.[10] Thus, high frequencies are the most problematic in low temperature experiments. The interference can arise either by capacitive, inductive, or radiative coupling. The most direct way is coupling via the wires going to the magnet. The best test of such a heat leak is of course the low temperature experiment itself, where even nW heat leaks can be detected. We used our current supply with a miniature ''dipstick'' dilution cryostat with a base temperature of 50 mK. No extra heat leak due to the opera-

tion of the supply was observed. Thus the heat leak has to be $\ll 1\ \mu$W, if the cooling power of the dilution unit is taken into account.

A less sensitive method is to use a spectrum analyzer in order to look for possible local electric or magnetic rf fields. A simple probe for magnetic fields can be made of a small loop of coaxial cable.[11] The measured spurious magnetic fields are shown in Fig. 9. The switching noise from the microcontroller extends to very wide band of frequencies. By moving the probe the maximum interference was confirmed to come from the MCU. The aluminum cover of the supply reduced the measured level by 20 dB. To observe the interference level in a typical experimental situation the supply was connected to a small superconducting magnet inside a storage dewar. Measured with a 4 cm coax loop, there was no visible interference from the current supply (see the lower frame in Fig. 9).

VIII. DISCUSSION

The 18-bit resolution used in our design is at the leading edge of the present semiconductor technology. Great care is necessary to retain this kind of resolution in the actual output current. The imperfections are caused either by digital errors or by analog voltages and currents. For example, the 18-bit up/down counter can see a false input at the clock signal and make one wrong count. After this the whole scale has been shifted by one bit. The programmable logic circuit turned out to be quite sensitive to such digital noise during the testing with the cover open. The high input impedance of the counter is the major reason for the problem. Even with the metallic enclosure tightly secured, a mechanical shock or sudden strong electric field may trigger the overvoltage in the state machine. The microcontroller, on the other hand, turned out to be more robust. This is to be expected since it has been designed to operate in harsh environments, e.g., in automotive applications. Also, design of the microcontroller is rather conservative compared to that of the programmable logic circuit ispLSI2032.

The electromagnetic radiation from the circuit can be divided into differential- and common-mode signals. The first one is created by a high frequency current loop,[11] e.g., induced by a clock signal. The second is due to the inevitable inductive coupling to the ground. This will have large enough impedance to make a wire connected to the hot end of the ground lead inductance to operate as an antenna. The differential mode is well suppressed by the aluminum enclosure. The common-mode signal may be conducted out along the cables leaving the cabinet. These include the main power cord, the computer interface and the current wires to the magnet. The last one is, of course, the most crucial since it goes directly to the low temperature experiment. In our supply we have tried to keep all the possible sources of interference far away from the current output. The microcontroller is optoisolated from it. The A/D converter is operating at a low frequency of 32.768 kHz. Thus, we believe that we are close to the practical minimum of interference in this kind of a design.

The integrated circuits employed are relatively new and represent the state-of-art at the moment of writing. The stability was measured to be $\pm 70\ \mu$A, i.e., the least significant bit of the D/A converter. This is the inherent uncertainty of such a digital device. The low frequency noise in 0.1–10 Hz band was only $30\ \mu A_{pp}$. Thus these numbers indicate that the overall accuracy is as good as can be expected for such an 18-bit D/A converter. The 18 bits mean a 4 ppm resolution of the full scale. We want to emphasize that the components were selected to make operation up to ± 10 A current possible. If a smaller current is sufficient, it is a good idea to scale R_{ref} accordingly to achieve the 4 ppm full-scale resolution. Many of the problems connected with the high output current become easier to handle. A Peltier heat pump was installed but not actually used to regulate the temperature of R_{ref}. Its use may become necessary if the output current is stepped by large amounts and the change in the temperature of R_{ref} causes a substantial error in the linearity.

ACKNOWLEDGMENTS

This work was supported by the Academy of Finland and by the Vilho, Yrjö, and Kalle Väisälä Foundation. The authors thank Timo Varpula for discussions.

[1] S. B. Ross, J. R. Davis, and J. Dutra, Rev. Sci. Instrum. **64**, 2379 (1993).
[2] M. I. Aalto, J. Phys. E **6**, 176 (1973).
[3] Danfysik A/S, P.O. Box 29, Møllehaven 31, DK-4040 Jyllinge, Denmark.
[4] M. W. Keller, J. M. Martinis, N. M. Zimmerman, and A. H. Steinbach, Appl. Phys. Lett. **69**, 1804 (1996).
[5] C. D. Motchenbacher and F. C. Fitchen, *Low-Noise Electronic Design* (Wiley, New York, 1973).
[6] Motorola Inc., M68HC11 Reference manual (1991).
[7] National Instruments Corp., NAT9914 Reference Manual (1994).
[8] Motorola Inc., M68HC11 PCbug11 User's Manual (1992).
[9] V. Ruutu, J. Koivuniemi, Ü. Parts, A. Hirai, and M. Krusius, Physica B **194–196**, 159 (1994).
[10] O. V. Lounasmaa, *Experimental Principles and Methods Below 1 K* (Academic, London, 1974).
[11] H. W. Ott, *Noise Reduction Techniques in Electronic Systems*, 2nd ed. (Wiley, New York, 1988).